Heliyon 10 (2024) e34978

Contents lists available at ScienceDirect

Heliyon

journal homepage: www.cell.com/heliyon

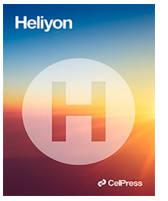

Research article

MicroRNA-486-3p affects cisplatin resistance in high-grade serous ovarian cancer by regulating TMIGD2: An experimental study

Jing Wang [b], Yanan Wu [a,*]

[a] Tarim University, Alaer, Xinjiang, China
[b] Xi'an Jiaotong University, Xi'an, Shaanxi, China

ARTICLE INFO

Keywords:
Ovarian cancer
Cisplatin resistance
miR-486-3p
TMIGD2

ABSTRACT

Ovarian cancer represents a major public health concern worldwide. High-grade serous ovarian cancer (HGSOC) is a primary epithelial ovarian cancer. Cisplatin resistance poses a substantial obstacle in the management of HGSOC, leading to unfavourable patient outcomes. The primary objective of this study was to investigate the mechanisms underlying cisplatin resistance in patients with HGSOC. TCGA data, GSE65819 dataset, and multiMiR package were used to identify 35 differentially expressed miRNAs (DE-miRNAs). Differentially expressed mRNAs (DE-mRNAs) are indicated using TCGA data. Further, weighted gene co-expression network analysis (WGCNA) was used to determine the correlation coefficients between the DE-mRNAs and DE-miRNAs. A network of miR-486-3p and TMIGD2 was constructed. Molecular biology experiments also indicated that low miR-486-3p or high TMIGD2 expression significantly increased the migratory rate and cisplatin resistance of both SK-OV3 and A2780 cells. In contrast, overexpression of miR-486-3p or downregulation of TMIGD2 decreased the migration rate and enhanced the sensitivity to cisplatin treatment, which provides insights for the development of novel therapeutic approaches. Moreover, RNA-binding protein immunoprecipitation experiment was used to determine the relationship between miR-486-3p and TMIGD2. Cell rescue assays were performed to further investigate these regulatory relationships. In TCGA and GSE65819 datasets, Benjamini and Hochberg false discovery rates (FDR) were selected for *P*-values. In the molecular biology experiments, one-way analysis of variance was employed to compare different groups, supplemented by Bonferroni post-hoc testing. Statistical significance was set at $p < 0.05$.

1. Introduction

Ovarian cancer is the fifth most common cause of cancer-related deaths in women worldwide, with approximately 313,959 new cases and 207,252 deaths reported in 2020 [1]. The subtype with the highest number of deaths among all types is high-grade serous ovarian cancer (HGSOC) [2]. The 5-year survival rate of patients with HGSOC due to chemotherapy resistance ranges from 35 % to 40 % [3]. The Gynecologic Cancer InterGroup (GCIG) recommends four platinum response classifications: platinum-refractory, platinum-resistant, partially platinum-sensitive, and platinum-sensitive disease [4]. The median survival of patients with platinum-resistant ovarian cancer is 9–12 months, and the response rate to subsequent chemotherapy is <15 %. Ultimately, almost all patients with HGSOC develop resistance to platinum [5]. Recently, considerable attention has been paid to unravelling the molecular

* Corresponding author.
E-mail address: wuyanan@taru.edu.cn (Y. Wu).

https://doi.org/10.1016/j.heliyon.2024.e34978
Received 16 April 2024; Received in revised form 15 July 2024; Accepted 19 July 2024
Available online 19 July 2024

mechanisms that drive drug resistance in ovarian cancer, with a particular focus on the role of miRNAs. miRNA research has emerged as a significant field of study to elucidate the intricate mechanisms underlying drug resistance in ovarian cancer [6].

MiR-486-3p, a specific miRNA, has garnered significant attention in cancer research because of its association with tumourigenesis and cancer progression. It is frequently downregulated in cancer tissues and its low expression correlates with poor prognosis and shorter overall survival across various cancer types. Extensive studies have explored the role of miR-486-3p in lung [7], colorectal [8], thyroid [9], hepatocellular [10], and pancreatic cancers [11], demonstrating its tumour-suppressive effects and potential clinical implications. Therefore, miR-486-3p is a promising target for cancer diagnosis, prognosis, and therapeutic intervention [12].

Similarly, TMIGD2 has also gained attention in cancer research as it is found to be over-expressed in multiple cancer types, including lung cancer [13], colorectal cancer [14], and hepatocellular carcinoma [15]. Higher TMIGD2 expression was associated with poor prognosis and shorter overall survival. Recent studies on the role of TMIGD2 in cancer have shed light on its potential as a target for future therapeutic strategies. Collectively, these findings emphasise the significance of miR-486-3p and TMIGD2 in cancer research and highlight their potential as targets for the diagnosis, prognosis, and therapeutic intervention in various cancer types. However, the role of miR-486-3p and TMIGD2 in drug resistance of ovarian cancer has not been reported and requires further investigation.

Our findings demonstrated cisplatin resistance in ovarian cancer and highlighted the potential of miR-486-3p and TMIGD2 as therapeutic targets for overcoming drug resistance in ovarian cancer.

2. Materials and methods

2.1. Bioinformatics mining methods

Differentially expressed mRNAs (DE-mRNAs) and miRNAs (DE-miRNAs) associated with ovarian cancer were identified by analysing a data series obtained from The Cancer Genome Atlas (TCGA), a publicly available database. Moreover, we downloaded the cases and file counts of TCGA-OV which separately contained miRNA-Seq and RNA-Seq data. In our analysis of ovarian cancer data from the TCGA database, we employed "edgeR" packages (Database Version: 3.28.1) to determine the DE-mRNAs and DE-miRNAs (foldchange = 1; pad = 0.05). EdgeR is a Bioconductor package designed to analyse digital gene expression data [16]. Volcano plots were used to visualise mRNA and miRNA expression.

Gene expression profiles of ovarian cancer (GSE65819) were retrieved from the Gene Expression Omnibus (GEO) database (https://www.ncbi.nlm.nih.gov/geo/) which selects samples from primary refractory, resistant, sensitive, and matched acquired resistant diseases. In the dataset GSE65819, which utilised the GPL19765 NanoString nCounter miRNA Human v2.1, samples were divided into four parts based on sources: ascitic fluid of HGSOC, the fallopian tube of normal, primary tumour of HGSOC, and tumour tissue from distant metastatic locations of HGSOC. Metastatic tumour tissue and ascitic fluid were not within the scope of the experimental research. Therefore, we analysed 7 normal samples and 80 samples of primary high-grade serous ovarian cancer tumours.

The multiMiR package (Database Version 2.3.0) gathered nearly 50 million records from 14 databases, more than any other collection. In this study, we used a database in the multiMiR package which includes three drugs/disease-related information (miR2Disease, Pharmaco miR, and PhenomiR) [17] to detect DE-miRNAs in ovarian cancer. Furthermore, the DE-miRNAs in TCGA, GSE65819, and multiMiR databases were compared using Venn plots to screen for shared miRNAs.

To further investigate the co-expression patterns relevant to ovarian cancer (OV) diagnosis, we performed weighted gene co-expression network analysis (WGCNA, Database Version 1.69) which provides R functions for weighted correlation network analysis [18]. Subsequently, a correlation network was constructed for the identified modules of interest using WGCNA and exported as an edge and node list file compatible with visualisation in Cytoscape (Database Version: 3.10.1). According to the Cytoscape results, we found three groups of miRNA and mRNA correlation networks, including EIF2S2P4 and miR-107, HMGN2P3 and miR-107, TMIGD2, and miR-486-3p. Moreover, EIF2S2P4 and HMGN2P3 are pseudogenes which are segments of DNA that structurally resemble a gene but are not capable of coding a protein [19]. Therefore, in our study, we selected the miR-486-3p single-regulatory TMIGD2 for further research.

UCSC XenaShiny is an R Shiny package used to search, download, explore, analyse, and visualise data from UCSC Xena data hubs [20]. We used XenaShiny (Database Version 1.1.9) to visualise the expression of TMIGD2 in different tumour tissues. The Kaplan–Meier (KM) plotter database contains data on TMIGD2 mRNA expression and prognostic parameters. Probes recommended for candidate checkpoint genes were selected for analysis.

In our study, all the databases belonged to public repositories. Ethical approval was obtained from all patients included in the database. Users can download the relevant data for free for research and publish relevant articles. Therefore, the authors declare there are no ethical issues or conflicts of interest.

2.2. Cell lines and culture

We procured two human epithelial ovarian cancer cell lines, SK-OV3 and A2780 (Fenghui Biology, China), and maintained them in MEM (Cytivad, USA). All cells were supplemented with 10 % foetal bovine serum (FBS, New Zealand) and 1 % penicillin-streptomycin (MedChemExpress, China), and maintained in a CO^2 incubator (Thermo Fisher Scientific) under appropriate conditions.

2.3. Lentiviral construction

High- and low-expression lentiviruses for miR-486-3p and TMIGD2 (Gene ID: 126,259) were obtained from Tsingke (China) and

OBiO Technology (China), respectively. To construct these lentiviruses, the miR-486-3p and TMIGD2 sequences were inserted into the lentiviral vector, Puro-CMV.

2.4. Establishment of stable cell lines

SK-OV3 and A2780 cells were seeded in six-well plates and incubated for 24 h. Subsequently, the cells were infected with recombinant lentiviruses and the transfected cells were cultured for 72 h. To select stable cell lines, puromycin (DEEYEE, China) was added to the culture medium at a concentration of 2 μg/ml. The medium containing puromycin was replaced every 2 days for 2 weeks to ensure the survival and proliferation of stable cell lines. Fluorescence microscopy was used to detect stable cell lines.

2.5. Total RNA isolation and quantification of miRNA expression

Total RNA was isolated from SK-OV3 and A2780 cells using the MolPure Cell/Tissue miRNA Kit (YEASEN, China). The RNA concentration and quality were assessed using a NanoDrop spectrophotometre (Thermo Scientific, USA). To synthesise the first-strand cDNA of miRNA, we used the Mir-X™miRNA First-Strand Synthesis Kit (TaKaRa, Japan). Synthesis was performed at 37 °C for 60 min, followed by a step at 85 °C for 5 s. In summary, following the manufacturer's guidelines, 500 ng of total RNA per sample was subjected to reverse transcription, resulting in 10 μL of cDNA. For miR-486-3p analysis, quantitative Real-time PCR (qRT-PCR) was performed using SYBR Premix Ex *Taq*II (TaKaRa Biotechnology, Japan). To normalise the expression levels, small nuclear RNA U6 was used as an endogenous control for miR-486-3p. Relative expression levels were determined using the $2^{-\triangle\triangle Ct}$ method, where normalisation was performed with respect to the control genes.

2.6. Western blotting

For whole-cell lysis, the cells were treated with RIPA buffer supplemented with a phosphatase inhibitor and protease inhibitor cocktail. Protein concentrations in the cell lysates were determined using a bicinchoninic acid (BCA) protein assay kit (Beyotime, China). Subsequently, cell protein lysates were subjected to 15 % sodium dodecyl sulfate-polyacrylamide gel electrophoresis (SDS-PAGE), followed by transfer onto polyvinylidene fluoride (PVDF) membranes (Millipore, USA). The membranes were then probed with specific antibodies, including anti-TMIGD2 (1:1000); Thermo Fisher Scientific (USA) and β-actin (1:1000); Proteintech (China). All bands were normalised to β-actin for quantification and analysis.

2.7. RNA-binding protein immunoprecipitation

The experiment was performed using an RNA-binding protein immunoprecipitation (RIP) Assay Kit (Bersin Bio, China). The RNA-binding protein was pulled down using a TMIGD2 antibody and the co-precipitated miR-486-3p was detected by qRT-PCR.

2.8. Wound healing assay

To assess the migratory capacity of OV cells, a wound-healing assay was performed. SK-OV3 and A2780 cells were seeded at a density of 80,000 cells in 500 μL of culture medium per well in a 6-well plate. The cells were allowed to grow until they reached confluence and formed a monolayer. Stable cell lines with TMIGD2 and miR-468-3p knockdown were established using the TMIGD2 shRNA lentivirus (OBiO Technology, China) and miR-468-3p shRNA lentivirus (Tsingke, China), respectively. Conversely, stable cell lines with upregulated expression of TMIGD2 and miR-468-3p were established using lentiviruses overexpressing TMIGD2 (OBiO Technology, China) and miR-468-3p (Tsingke, China). After 6 h of transfection, a linear scratch was made in the centre of each well using a sterile 200 μL pipette tip. Subsequently, floating cells were removed by washing with 1× PBS, followed by the addition of 500 μL of low-serum growth medium (3 % FBS in MEM) per well. Cell migration was monitored by capturing images using a light microscope at 0, 24, and 48 h post-wound formation. The migration rate was determined by measuring the initial gap length (0 h) and residual gap length (24 and 48 h) using the ImageJ software.

2.9. Cell counting kit-8 (CCK8) assay

To evaluate the cisplatin resistance of SK-OV3 and A2780 cells, the CCK8 kit (DEEYEE, China) was used. Transfected SK-OV3 and A2780 cells were seeded in 96-well plates and treated with 2 μg/ml cisplatin for 24 h. Following treatment, the cells were incubated with 10 μl of CCK8 reagent for 2 h. Cell viability was subsequently assessed by measuring the absorbance at a wavelength of 450 nm.

2.10. Statistical analysis

In TCGA and GSE65819 datasets, the Benjamini & Hochberg false discovery rate (FDR) was selected for *p*-values which provided a balance between the discovery of statistically significant genes and the limitation of false positives. Statistical significance was set at $p < 0.05$. The results of the molecular biology experiments are presented as mean ± standard error of the mean (SEM). Statistical analyses were conducted using the GraphPad Prism 5 software. One-way analysis of variance (ANOVA) was used to compare different groups, supplemented by the Bonferroni post-hoc test. Statistical significance was determined at $p < 0.05$ and expressed using the

following notation: $^{*}p < 0.05$, $^{**}p < 0.01$ and $^{***}p < 0.001$;$^{\#\#}p < 0.01$ and $^{\#\#\#}p < 0.001$;$^{\$}p < 0.05$ and $^{\$\$\$}p < 0.001$;$^{\hat{}}p < 0.05$ and $^{\hat{}\hat{}\hat{}}p < 0.001$;$^{\&\&}p < 0.01$ and $^{\&\&\&}p < 0.001$.

3. Results

3.1. Identification of DE-mRNAs and DE-miRNAs

Through our analysis of TCGA data, we observed significant differential expressions of 5085 mRNAs (Fig. 1A) and 557 miRNAs (Fig. 1B). Additionally, a comparative analysis between seven normal samples and 80 primary high-grade serous cancer samples from GSE65819 identified a dataset of DE-miRNAs using the adj.$p < 0.05$. This dataset comprises 238 DE-miRNAs, shedding light on specific miRNA alterations associated with high-grade serous cancer (Fig. 1C). We identified a dataset of DE-miRNAs by applying an adjusted $p < 0.05$. To compare the DE-miRNAs identified from different sources, including TCGA database, GSE65819, and multiMiR databases, Venn diagrams screened 35 overlapping miRNAs, including hsa-miR-429, hsa-miR-27a-3p, hsa-miR-223-3p, hsa-miR-199b-5p, hsa-miR-340-5p, hsa-miR-126-3p, hsa-miR-221-3p, hsa-miR-183-5p, hsa-miR-451a, hsa-miR-143-3p, hsa-miR-141-3p, hsa-miR-10b-5p, hsa-miR-200c-3p, hsa-miR-142-3p, hsa-miR-30b-5p, hsa-miR-181c-5p, hsa-miR-214-3p, hsa-miR-18a-5p, hsa-miR-20a-5p, hsa-miR-146b-5p, hsa-miR-96-5p, hsa-miR-193a-3p, hsa-miR-26b-5p, hsa-miR-23b-3p, hsa-miR-21-5p, hsa-miR-130b-3p, hsa-miR-15a-5p, hsa-miR-182-5p, hsa-miR-301a-3p, hsa-miR-486-3p, hsa-let-7g-5p, hsa-let-7b-5p, hsa-miR-107, hsa-miR-224-5p, hsa-miR-155-5p and observed that they were shared among these datasets (Fig. 1D). A recent study also found that many of these miRNAs were associated with platinum chemoresistance and its effective treatment of resistant OV including miR-200c, miR-141, miR-429, miR-21, let-7b [21], miR-183-5p [22], miR-182 [23], miR-15a [24], miR-221, miR-223, miR-27a [25]. WGCNA was used to detect the correlation coefficient between DE-mRNAs and DE-miRNAs, with a correlation coefficient >0.65 (Fig. 1E). A network was constructed between the DE-miRNAs and DE-mRNAs, which were identified using WGCNA. The resulting network was visualised using Cytoscape (Fig. 1F). Three groups of miRNA and mRNA correlation networks were constructed as follows: EIF2S2P4 and miR-107, HMGN2P3 and miR-107, and TMIGD2 and miR-486-3p. EIF2S2P4 and HMGN2P3 are pseudogenes which do not code for proteins [19]. In addition,

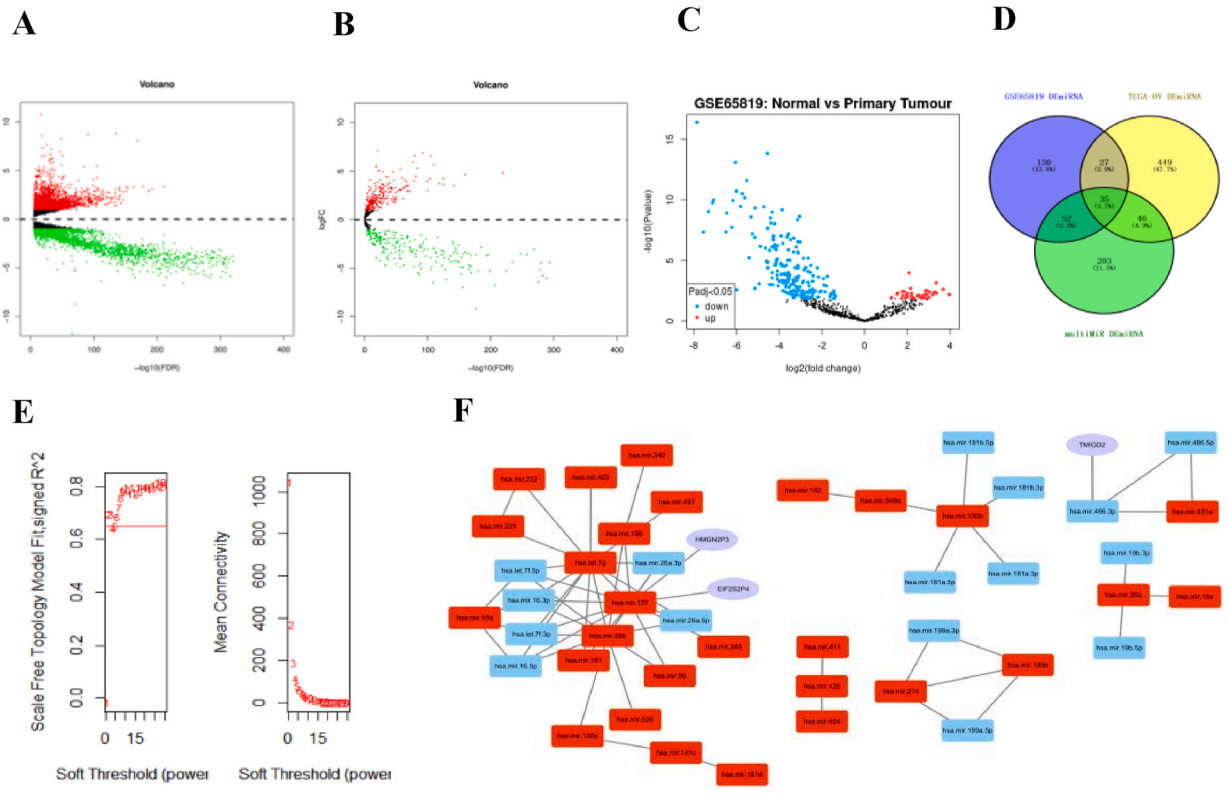

Fig. 1. The comprehensive bioinformatics analysis of the TCGA database, GSE65819, and multiMiR in ovarian cancer (A) The analysis of the TCGA database for ovarian cancer revealed the presence of 5085 DE-mRNAs that are associated with the disease. (B) The presence of 557 DE-miRNAs was associated with ovarian cancer in the TCGA database. (C) The analysis of the GSE65819 database indicated that the presence of 238 DE-miRNAs was associated with ovarian cancer. (D) Comparison of differential miRNAs using Venn plots to screen for shared miRNAs.(E) WGCNA was used to detect the correlation coefficient between DE-mRNAs and DE-miRNAs of TCGA database, with a correlation coefficient greater than 0.65 (F) The network between DE-miRNAs and DE-mRNAs were selected by WGCNA and visualised in Cytoscape. Supplementary Table 1 indicates the multiMiR results in ovarian cancer.

previous studies have identified that miR-486-3p is associated with multiple tumour drug resistance [7,10,26], and that TMIGD2 participates in the mechanisms of tumour-intrinsic and -extrinsic resistance and has become a new therapeutic target for cancer therapy [27]. Finally, the remarkable regulatory relationship observed between miR-486-3p and TMIGD2 highlights its potential significance and warrants further investigation in subsequent steps.

3.2. Bioinformatics analysis of miR-486-3p and TMIGD2

By analysing the GSE65819 dataset, we compared normal and cancer groups and found a significant decrease in the expression of miR-486-3p in ovarian cancer (Fig. 2A). KM plotter analysis revealed a compelling association between low miR-486 expression and significantly shortened survival in many cancers, including bladder carcinoma, kidney renal clear cell carcinoma, kidney renal papillary cell carcinoma, lung adenocarcinoma, lung squamous cell carcinoma, pancreatic ductal adenocarcinoma, and stomach adenocarcinoma. However, there was no statistically significant difference in the KM mapping analysis of ovarian cancer. To assess the prognostic significance of TMIGD2 expression, we used the KM plotter, an established tool for survival analysis. In our analysis using XenaShiny, we observed a significant increase in TMIGD2 expression, specifically in OV cells (Fig. 2B). KM plotter analysis revealed a compelling association between high TMIGD2 expression and significantly shortened survival (Fig. 2C).

3.3. Verification of stable cell lines of lentivirus

To explore the role of miR-486-3p and TMIGD2 in OV, we conducted transfection experiments using high-expression and low-expression lentiviruses for miR-486-3p and TMIGD2 in SK-OV3 and A2780 cell lines. To determine the transfection of high- and low-expression lentiviruses for miR-486-3p and TMIGD2, qRT-PCR and western blotting (WB) were used to assess the efficacy of stable cell line formation. One-way ANOVA was used to compare different groups, supplemented by the Bonferroni post-hoc test. Statistical significance was set at $p < 0.05$. We observed a notable decrease ($p < 0.001$) in the expression of miR-486-3p (Fig. 3A), validating the successful generation of low-expression cell lines. Conversely, we observed a significant increase ($p < 0.001$) in the expression levels of miR-486-3p (Fig. 3B), confirming the successful establishment of high-expression cell lines. Additionally, our analysis revealed a significant decrease ($p < 0.001$) in the expression level of TMIGD2 (Fig. 3C), providing evidence for the successful generation of low-expression cell lines. Conversely, we observed a significant increase ($p < 0.001$) in the expression levels of TMIGD2 (Fig. 3C), confirming the successful establishment of high-expression cell lines. Furthermore, we confirmed the successful establishment of stable cell lines by combining the fluorescence microscopy results (Fig. 3D and E).

3.4. The regulation between miR-486-3p and TMIGD2

One-way ANOVA was used to compare different groups, supplemented by the Bonferroni post-hoc test. Statistical significance was set at $p < 0.05$. In SK-OV3 cells with low expression of miR-486-3p, we observed the upregulation of TMIGD2 through Western blot analysis ($p < 0.01$) (Fig. 4A). Conversely, in SK-OV3 cells with high miR-486-3p expression, we detected downregulation of TMIGD2 ($p < 0.05$) (Fig. 4A). Similarly, in A2780 cells with low miR-486-3p expression, we observed an upregulation of TMIGD2 ($p < 0.05$)

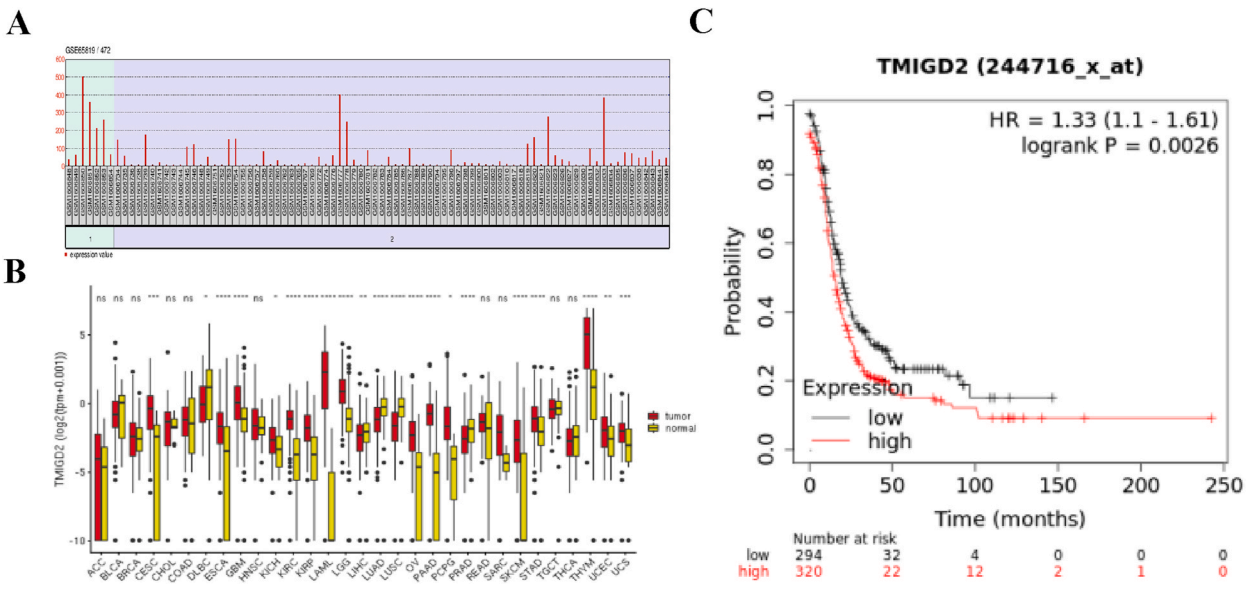

Fig. 2. Bioinformatics analysis of miR-486-3p and TMIGD2 (A) The analysis of the GSE65819 for miR-486-3p. (B) The analysis of the XenaShiny for TMIGD2 (C) The KM plotter of TMIGD2.

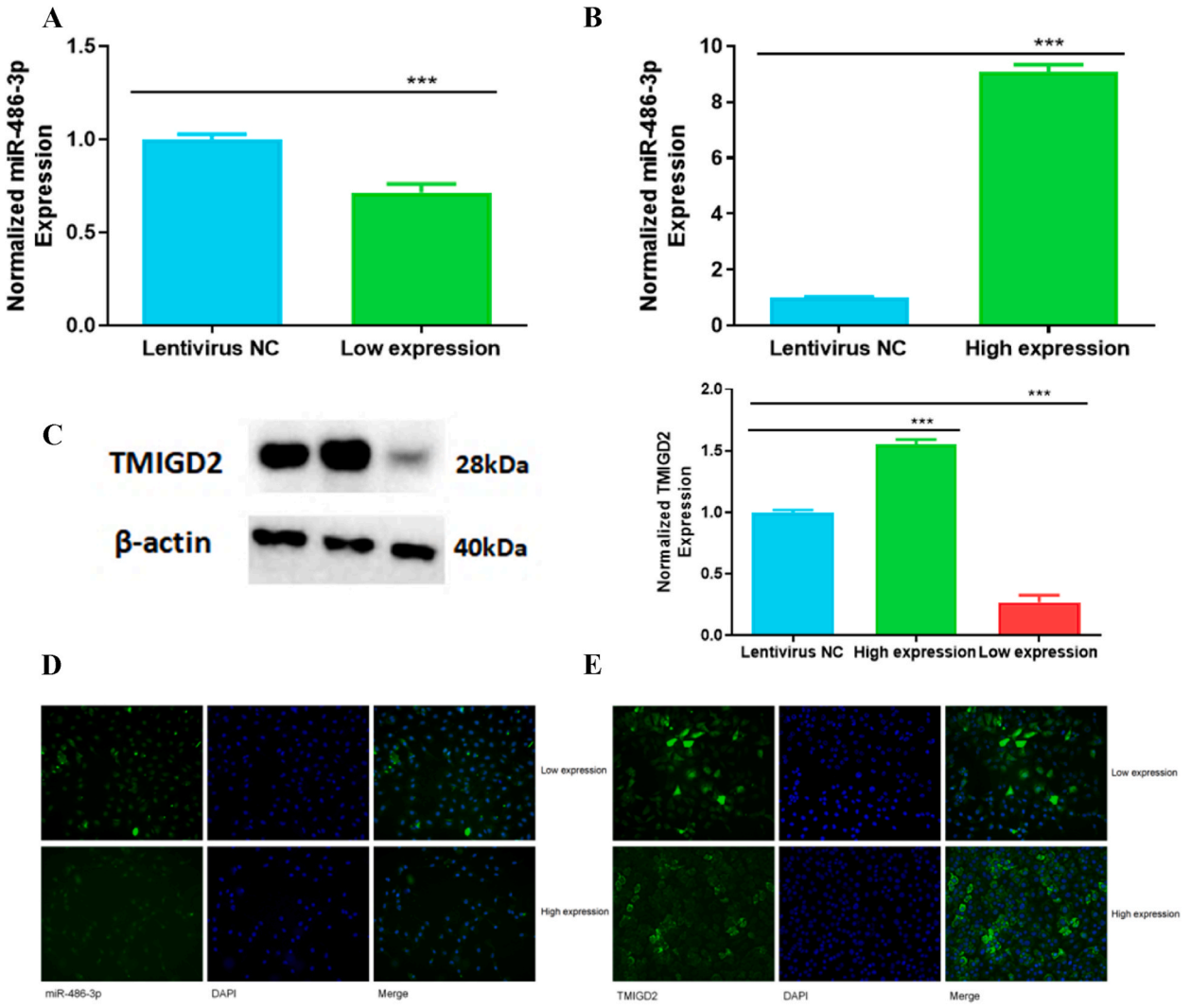

Fig. 3. Verifying the stable cell lines containing high-expression or low-expression lentiviruses (A) The q-PCR was used to detect the expression of the low-expression miR-486-3p. (B) The q-PCR was used to detect the expression of the high-expression miR-486-3p. (C) The WB was used to detect the expression of the high-expression or low-expression TMIGD2 (The original images is provided in the Supplementary Fig. 3 TMIGD2 and Supplementary Fig. 3 actin). (D, E) A fluorescence microscope was employed to detect the stable cell lines.

(Fig. 4B), whereas in A2780 cells with high expression of miR-486-3p, we observed downregulation of TMIGD2 ($p < 0.01$) (Fig. 4B). The RNA-binding protein immunoprecipitation results revealed a significant interaction between the regulatory elements of miR-486-3p and TMIGD2 in the SK-OV3 ($p < 0.05$) and A2780 cell lines ($p < 0.01$) (Fig. 5).

3.5. The impact of miR-486-3p and TMIGD2 on the migration of SK-OV3 and A2780 cells

In our functional assays, we conducted migration experiments at two time points: 24 and 48 h. Additionally, all experimental groups were compared with the lentivirus-negative control (NC) group. Low expression of miR-486-3p resulted in enhanced migration of SK-OV3 and A2780 cells at 24 and 48 h compared to the control group. Conversely, high miR-486-3p expression led to reduced migration of both cell lines at 24 and 48 h (Fig. 6A and C). Furthermore, the manipulation of TMIGD2 expression showed significant trends, where low TMIGD2 expression correlated with decreased migration of SK-OV3 and A2780 cells at 24 and 48 h compared to that of the control group, whereas high TMIGD2 expression correlated with increased migration of SK-OV3 and A2780 cells at 24 and 48 h compared to that of the control group (Fig. 6B and D). One-way ANOVA was used to compare different groups, supplemented by the Bonferroni post-hoc test. Statistical significance was set at $p < 0.05$. Migration data were analysed using GraphPad Prism 5, which revealed interesting findings regarding the effects of miR-486-3p expression on SK-OV3 and A2780 cell growth. In SK-OV3 cells, low miR-486-3p expression significantly enhanced cell growth at both 24 ($p < 0.001$) and 48 h ($p < 0.01$). Conversely, high expression of miR-486-3p significantly inhibited cell growth at 24 ($p < 0.001$) and 48 h ($p < 0.001$) (Fig. 6E). Similarly, in A2780 cells, low miR-486-

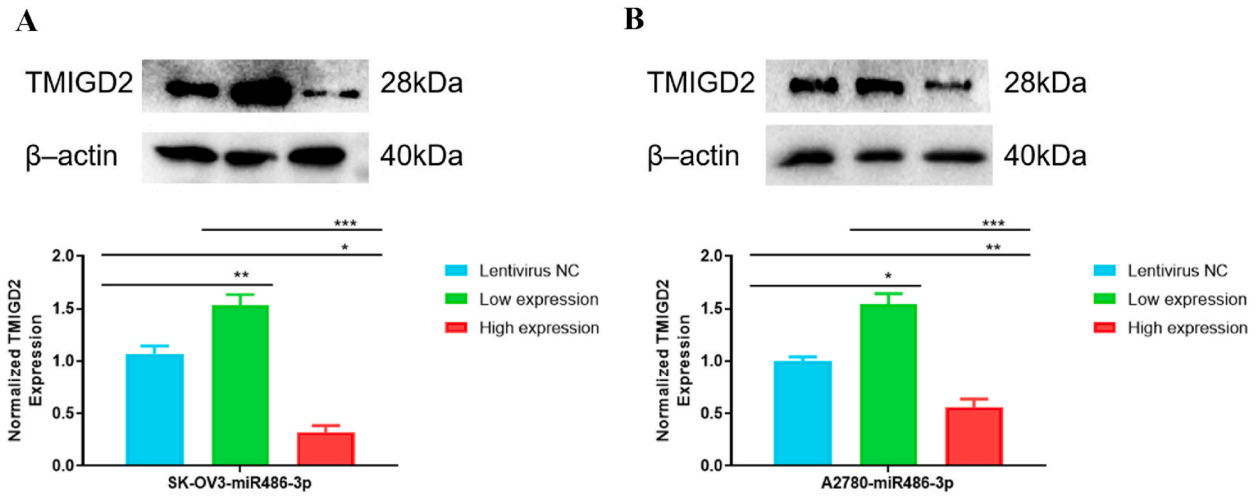

Fig. 4. MiR-486-3p regulated TMIGD2 (A) The expression changes of TMIGD2 through low or high expression of miR-486-3p on SK-OV3 cells (The original images were provided in the Supplementary Fig. 4 TMIGD2 and Supplementary Fig. 4 actin). (B) The expression changes of TMIGD2 through the low or high expression of miR-486-3p on A2780 cells (The original images were provided in the Supplementary Fig. 4 TMIGD2 and Supplementary Fig. 4 actin).

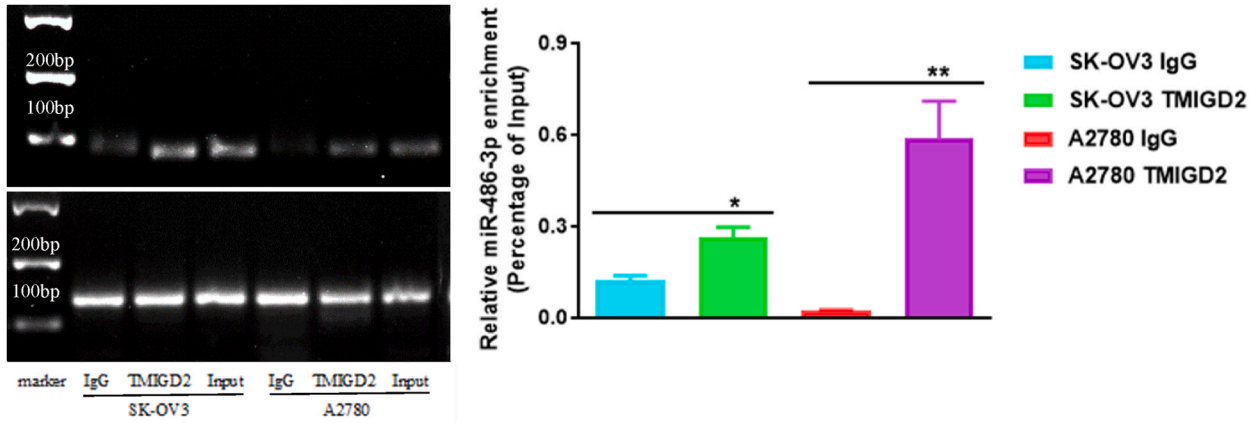

Fig. 5. A significant interaction between miR-486-3p and TMIGD2 (The original images is provided in the Supplementary Fig. 5 miR-486-3p and Supplementary Fig. 5 U6).

3p expression significantly enhanced cell growth at 24 ($p < 0.01$) and 48 h ($p < 0.001$). Conversely, high expression of miR-486-3p significantly inhibited cell growth at 24 ($p < 0.001$) and 48 h ($p < 0.05$) (Fig. 6G). In addition, TMIGD2 expression significantly affected cell migration. In SK-OV3 cells, low TMIGD2 expression significantly inhibited cell growth at both 24 ($p < 0.001$) and 48 h ($p < 0.001$). Conversely, high TMIGD2 expression significantly enhanced cell growth at 24 ($p < 0.001$) and 48 h ($p < 0.001$) (Fig. 6F). Similarly, in A2780 cells, low TMIGD2 expression significantly inhibited cell growth at 24 ($p < 0.05$) and 48 h ($p < 0.001$). Conversely, high TMIGD2 expression significantly enhanced cell growth at 24 ($p < 0.01$) and 48 h ($p < 0.001$) (Fig. 6H).

3.6. The impact of miR-486-3p and TMIGD2 on cisplatin-resistance in SK-OV3 and A2780 cells

The effects of miR-486-3p and TMIGD2 on cisplatin resistance were determined in SK-OV3 and A2780 cells. One-way ANOVA was used to compare different groups, supplemented by the Bonferroni post-hoc test. Statistical significance was set at $p < 0.05$. In the CCK8 assay, we observed that low miR-486-3p expression led to a decrease in the inhibitory rate of both SK-OV3 ($p < 0.001$) and A2780 ($p < 0.05$) cells against cisplatin (Fig. 7A and C). Conversely, high expression of miR-486-3p enhanced the inhibitory effects of cisplatin on SK-OV3 ($p < 0.001$) and A2780 ($p < 0.05$) cell viability (Fig. 7A and C). Furthermore, we observed that low TMIGD2 expression increased the inhibitory rate in both SK-OV3 ($p < 0.01$) and A2780 ($p < 0.01$) cells treated with cisplatin (Fig. 7B and D). Conversely, high TMIGD2 expression attenuated the inhibitory effects of cisplatin on SK-OV3 ($p < 0.05$) and A2780 cell viability ($p < 0.05$) (Fig. 7B and D). These results indicate that decreased levels of miR-486-3p or increased levels of TMIGD2 are associated with reduced sensitivity of OV cells to the inhibitory effects of cisplatin. Conversely, elevated miR-486-3p or decreased TMIGD2 levels

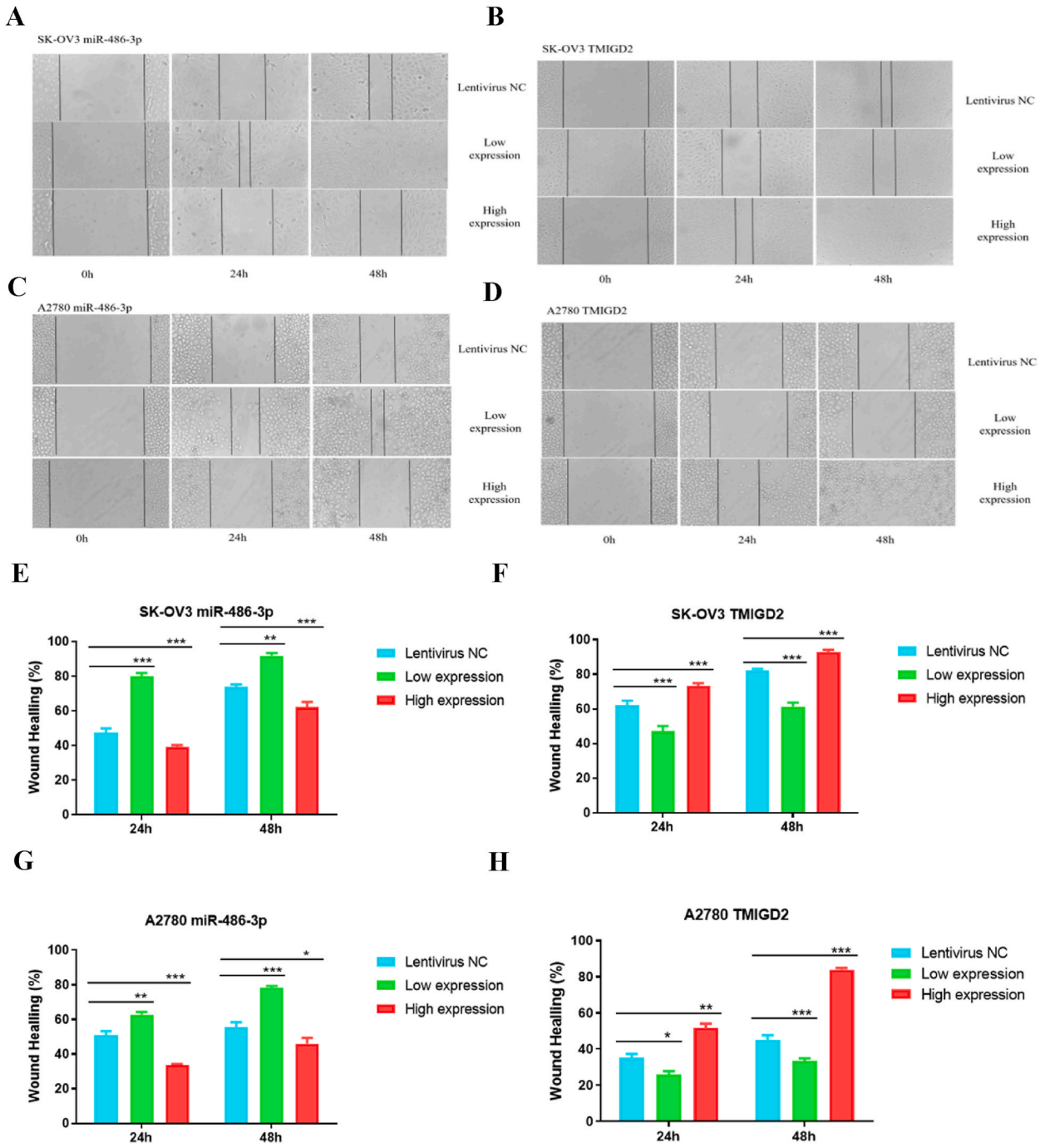

Fig. 6. The results of wound-healing assay (A) Migration activity determined by wound-healing assay at 24 and 48 h after transfection with high-expression or low-expression lentiviruses of miR-486-3p on SK-OV3 cells. (B) Migration activity was determined by wound-healing assay at 24 and 48 h after transfection with high-expression or low-expression lentiviruses of TMIGD2 on SK-OV3 cells. (C) Migration activity was determined by wound-healing assay at 24 and 48 h after transfection with high-expression or low-expression lentiviruses of miR-486-3p on A2780 cells. (D) Migration activity was determined by wound-healing assay at 24 and 48 h after transfection with high-expression or low-expression lentiviruses of TMIGD2 on A2780 cells. (E) Statistical results of Figure A. (F) Statistical results of Figure B. (G) Statistical results of Figure C. (H) Statistical results of Figure D.

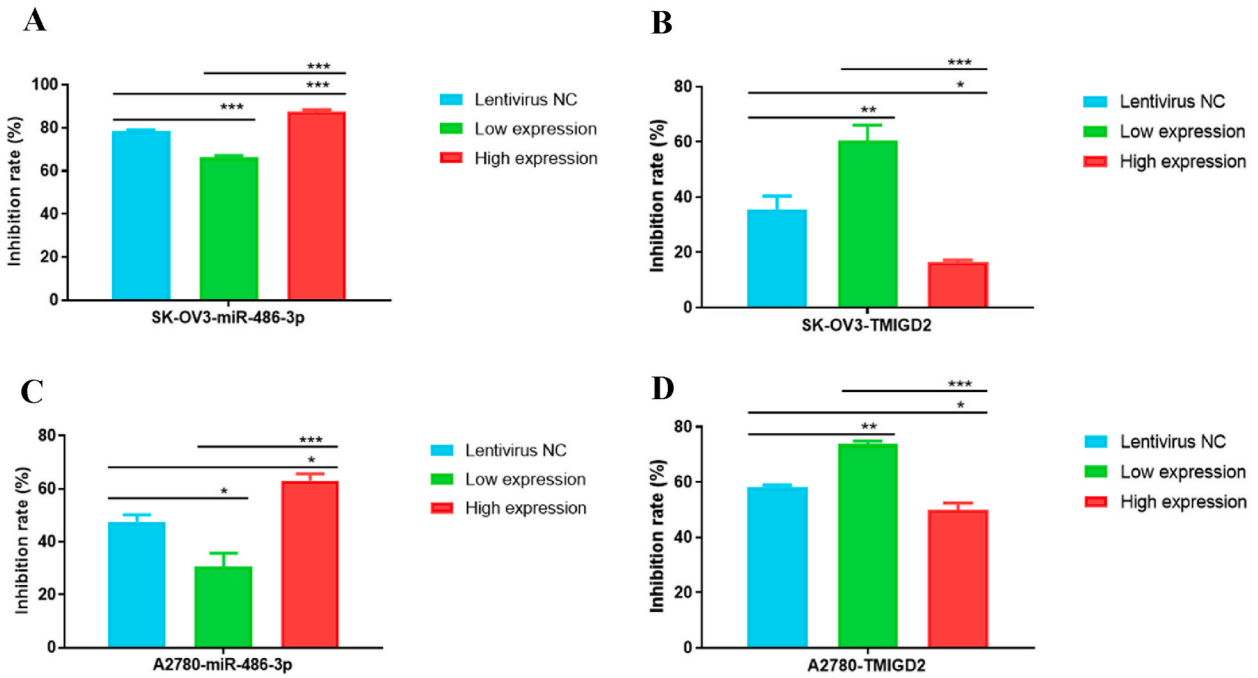

Fig. 7. The CCK-8 results were used to determine the effects of miR-486-3p and TMIGD2 on SK-OV3 and A2780 cells (A) The impact of miR-486-3p on SK-OV3 cells. (B) The impact of TMIGD2 on SK-OV3 cells (C) The impact of miR-486-3p on A2780 cells (D) The impact of TMIGD2 on A2780 cells.

increased the inhibitory effects of cisplatin.

3.7. TMIGD2 reverses the miR-486-3p-induced effects in SK-OV3 and A2780 cells

Rescue assays were performed using SK-OV3 and A2780 cells to investigate whether miR-486-3p exerts its biological effects through TMIGD2. Subsequently, the wound healing (Fig. 8A and B), and CCK8 assays (Fig. 9A and B) demonstrated that both high and low expression of TMIGD2 reversed the migration effect and drug resistance induced by miR-486-3p, suggesting the involvement of TMIGD2 in mediating the effects of miR-486-3p on the migration capability and drug resistance.

In summary, these results indicate that miR-486-3p potentially regulates TMIGD2 expression and plays a crucial role in altering the sensitivity of OV cells to cisplatin. Increasing miR-486-3p expression or reducing TMIGD2 expression can alleviate the migration capability and drug resistance.

4. Discussion

Ovarian cancer is a significant global public health concern, as highlighted by alarming statistics provided by the World Health Organization. In 2020 alone, an estimated 313,959 new cases and 207,252 deaths were reported worldwide due to this devastating disease [1]. Approximately 70 % of these patients are diagnosed with advanced-stage disease. Despite receiving standard care, most patients experience chemotherapy resistance, resulting in a global 5-year survival rate of approximately 30%–40 %. The main resistance mechanisms in ovarian cancer include abnormalities in transmembrane transport, alterations in DNA damage repair, dysregulation of cancer-associated signalling pathways, and epigenetic modifications. DNA methylation, histone modification, and non-coding RNA activity are important components of epigenetic modifications [28]. MiRNAs are small and highly conserved non-coding RNA molecules that exert a significant influence on ovarian cancer resistance [29]. Their ability to regulate gene expression and modulate key biological pathways contributes to cisplatin resistance of ovarian cancer cells. Recognising the gravity of this situation, we conducted this research to elucidate the mechanisms underlying drug resistance in ovarian cancer.

In this study, we initially identified DE-mRNAs and DE-miRNAs associated with ovarian cancer by analysing a dataset obtained from the publicly available TCGA database. To further validate these findings, we utilised the GSE65819, GSE239685, and multiMiR datasets to confirm the expression patterns of DE-miRNAs identified in the TCGA database. This approach strengthened the robustness of our findings and enhanced the reliability of the identified DE-miRNAs associated with ovarian cancer. Recent studies have shown that misalignment and splicing events in miRNAs promote carcinogenesis and drug resistance in leukaemia and breast, cervical, prostate, colorectal, and ovarian cancers. miRNAs may affect the drug affinity of target proteins, ultimately leading to drug resistance [30]. Protein-RNA interactions play structural, catalytic, and regulatory roles in cells, and immunoprecipitation assays are used to study RNA-protein interactions *in vivo*. The RIP method utilises the highly reactive and reversible crosslinking agent, formaldehyde,

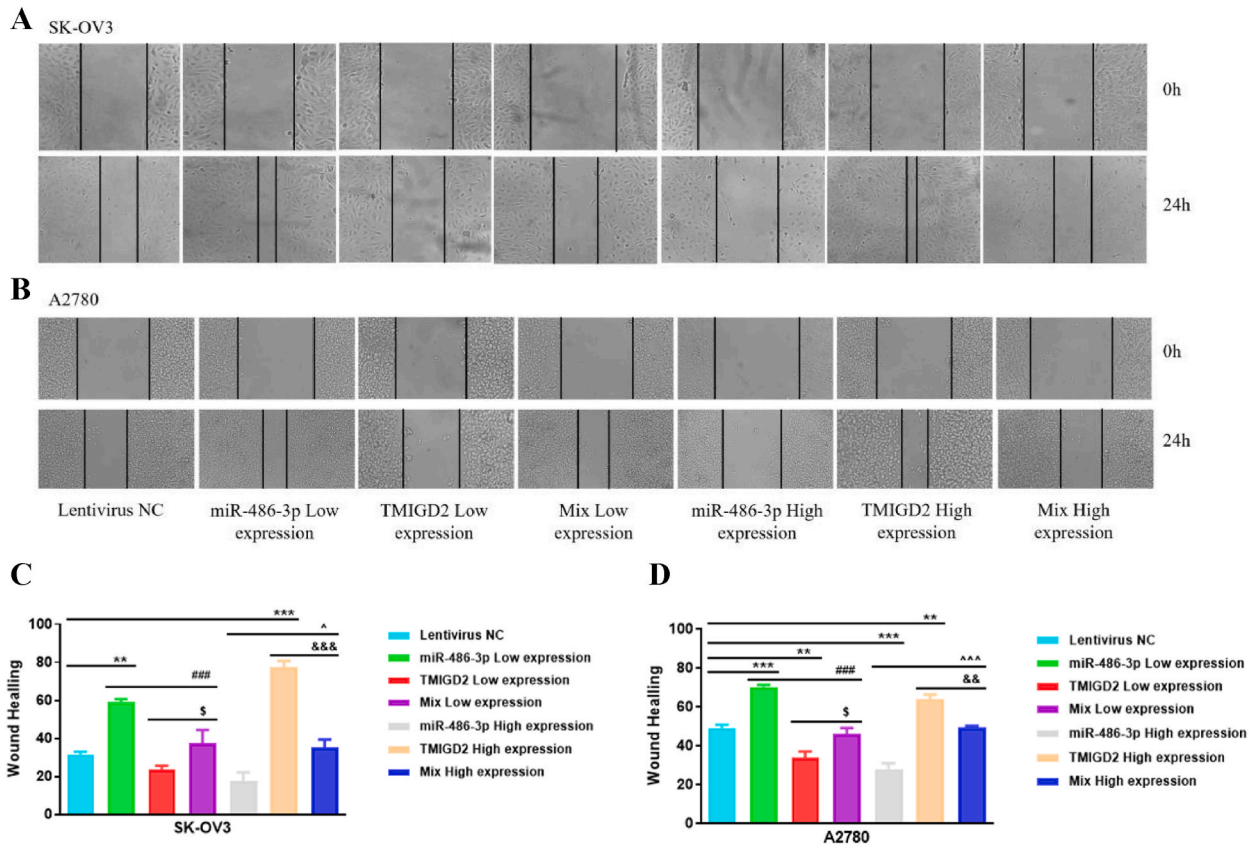

Fig. 8. The results of wound-healing assay in cell rescue assay (A) Migration activity determined by wound-healing assay at 24 h after transfection with high-expression or low-expression lentiviruses of miR-486-3p and TMIGD2 on SK-OV3 cells. (B) Migration activity was determined by wound-healing assay 24 h after transfection with high-expression or low-expression lentiviruses of miR-486-3p and TMIGD2 on A2780 cells. (C) Statistical results of Figure A. (D) Statistical results of Figure B.

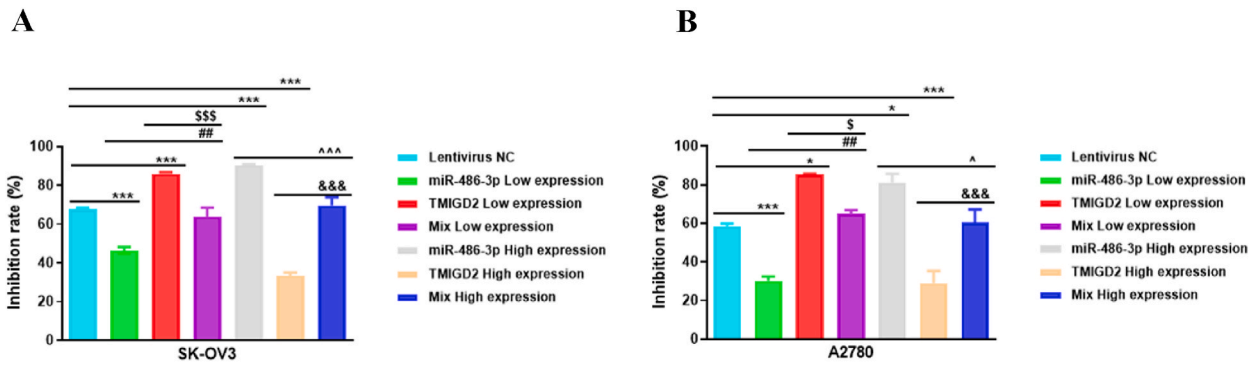

Fig. 9. The results of CCK-8 in cell rescue assay (A) The impact of high-expression or low-expression lentiviruses of miR-486-3p and TMIGD2 on SK-OV3 cells. (B) The impact of high-expression or low-expression lentiviruses of miR-486-3p and TMIGD2 on A2780 cells.

combined with highly rigorous immunoprecipitation to identify specific RNA associated with proteins. Similarly, our results revealed a remarkable regulatory relationship between miR-486-3p and TMIGD2 using the RIP assay [31]. Furthermore, our study revealed that SK-OV3 and A2780 cells with high miR-486-3p expression showed downregulation of TMIGD2, whereas cells with low miR-486-3p expression showed upregulation of TMIGD2 expression. Rescue assays were performed to determine the involvement of TMIGD2 in mediating the effects of miR-486-3p on migration capability and drug resistance.

Recently, many studies have found that miR-486-3p acts as a functional regulatory miRNA with aberrant expression in several different cancers; for example, miR-486-3p expression was found to be downregulated in oral squamous cell carcinoma [32], cervical

cancer [33] and lung cancer [34]. Furthermore, our study revealed that low miR-486-3p expression increased the migration rate of SK-OV3 and A2780 cells. Multidrug resistance (MDR) is one of the primary factors that causes treatment failure in patients receiving cancer chemotherapy. Several studies have suggested that miRNAs play a pivotal role in certain MDR cancer cells by affecting development, differentiation, growth, cell apoptosis, stress response, and T-cell homeostasis. miRNAs are RNA transcripts that do not have protein-coding functions but target gene expression by guiding the RNA-induced silencing complex to recognise the target mRNA to either suppress its translation or cause its cleavage [35]. Previous studies indicated that miR-486-3p is downregulated in sorafenib-resistant cells [10]. In addition, our study confirmed that low miR-486-3p expression was associated with increased resistance to ovarian cancer.

Mortezaee highlighted the potential of TMIGD2 as a target for the development of agonistic bispecific antibodies to counteract tumour resistance to programmed death-1 (PD-1)/PD-L1 blockade therapy [36]. Similarly, our findings demonstrate that increased TMIGD2 expression and high TMIGD2 levels are associated with significantly shorter survival outcomes. This observation aligns with previous studies that reported elevated TMIGD2 expression in other cancer types, such as astrocytoma, IDH-1 mutations, and low-grade and young patients with glioma [37]. Furthermore, a previous study indicated that TMIGD2 expression in human colon cancer cell lines is associated with increased resistance of tumour cells to the cytotoxic effects of the chemotherapeutic agent doxorubicin [38]. TMIGD2 is a membrane glycoprotein belonging to the immunoglobulin superfamily that is involved in the activation, inhibition, and fine-tuning of the T-cell immune response. Immune responses play a central role in tumour development and treatment resistance [39]. Consistent with previous studies, our results confirmed that high expression of TMIGD2 was associated with a reduction in the sensitivity of ovarian cancer cells to the inhibitory effects of cisplatin.

This study has some limitations. First, the data used in the study came from publicly available databases, which may have introduced some degree of selection bias into the results. Second, the datasets of cisplatin resistance in ovarian cancer did not have large sample sizes, which may have limited the statistical accuracy of the data analysis. Further studies are necessary to explore the roles of miR-486-3p and the TMIGD2 network in ovarian cancer in nude mice. Additionally, because TMIGD2 acts on tumour drug resistance by regulating immune responses, the next step would be determining the type of T cells specifically activated by TMIGD2.

In conclusion, we found that increasing miR-486-3p or reducing TMIGD2 expression can alleviate the migration capability and drug resistance, revealing new treatment targets in ovarian cancer. Moreover, the miR-486-3p–TMIGD2 regulatory network may represent a future immunotherapeutic pathway for drug-resistant ovarian cancer.

5. Conclusions

We employed a comprehensive approach that combined bioinformatics and molecular biology techniques to investigate the effects of miR-486-3p and TMIGD2 on cisplatin resistance in ovarian cancer cells. Our results demonstrate that miR-486-3p potentially regulates TMIGD2 expression and plays a crucial role in altering the sensitivity of ovarian cancer cells to cisplatin treatment. This integrated approach provides valuable insights into the molecular mechanisms underlying cisplatin resistance in ovarian cancer and highlights the potential of miR-486-3p and TMIGD2 as therapeutic targets to overcome drug resistance in ovarian cancer.

Ethics approval and consent to participate

Not applicable.

Patient consent for publication

Not applicable.

Funding

This study was supported by the Research Project of the President Fund of Tarim University, Tarim University, China (grant number: TDZKSS202204).

Data availability statement

The clinical data were from publicly available online datasets. The online sites: TCGA: https://www.cancer.gov/; GEO: https://www.ncbi.nlm.nih.gov/geo/; UCSC XenaShiny: https://shiny.hiplot.cn/ucsc-xena-shiny/. The research data associated with this article is not deposited in the publicly available repository. The data for this article will be made available by the authors, and further inquiries can be directed to the corresponding author.

CRediT authorship contribution statement

Jing Wang: Writing – original draft, Visualization, Software, Methodology. **Yanan Wu:** Writing – review & editing, Project administration, Investigation, Funding acquisition, Formal analysis, Data curation.

Declaration of competing interest

The authors declare that they have no known competing financial interests or personal relationships that could have appeared to influence the work reported in this paper.

Appendix A. Supplementary data

Supplementary data to this article can be found online at https://doi.org/10.1016/j.heliyon.2024.e34978.

References

[1] H. Sung, J. Ferlay, R.L. Siegel, M. Laversanne, I. Soerjomataram, A. Jemal, F. Bray, Global cancer statistics 2020: GLOBOCAN estimates of incidence and mortality worldwide for 36 cancers in 185 countries, CA A Cancer J. Clin. 71 (2021) 209–249.
[2] Integrated genomic analyses of ovarian carcinoma, Nature 474 (2011) 609–615.
[3] D. Holmes, Ovarian cancer: beyond resistance, Nature 527 (2015) S217.
[4] G.C. Stuart, H. Kitchener, M. Bacon, A. duBois, M. Friedlander, J. Ledermann, C. Marth, T. Thigpen, E. Trimble, Gynecologic cancer InterGroup (GCIG) consensus statement on clinical trials in ovarian cancer: report from the fourth ovarian cancer consensus conference, Int. J. Gynecol. Cancer 21 (2011) (2010) 750–755.
[5] A. Davis, A.V. Tinker, M. Friedlander, "Platinum resistant" ovarian cancer: what is it, who to treat and how to measure benefit? Gynecol. Oncol. 133 (2014) 624–631.
[6] L. Salmena, L. Poliseno, Y. Tay, L. Kats, P.P. Pandolfi, A ceRNA hypothesis: the Rosetta Stone of a hidden RNA language? Cell 146 (2011) 353–358.
[7] H.H. Kwok, Z. Ning, P.W. Chong, T.S. Wan, M.H. Ng, G.Y.F. Ho, M.S. Ip, D.C. Lam, Transfer of extracellular vesicle-associated-RNAs induces drug resistance in ALK-translocated lung adenocarcinoma, Cancers 11 (2019).
[8] N. Mosakhani, V.K. Sarhadi, I. Borze, M.L. Karjalainen-Lindsberg, J. Sundström, R. Ristamäki, P. Osterlund, S. Knuutila, MicroRNA profiling differentiates colorectal cancer according to KRAS status, Genes Chromosomes Cancer 51 (2012) 1–9.
[9] L. Chen, L. Xiong, S. Hong, J. Li, Z. Huo, Y. Li, S. Chen, Q. Zhang, R. Zhao, J.A. Gingold, X. Zhu, W. Lv, Y. Li, S. Yu, H. Xiao, Circulating myeloid-derived suppressor cells facilitate invasion of thyroid cancer cells by repressing miR-486-3p, J. Clin. Endocrinol. Metab. 105 (2020).
[10] L. Ji, Z. Lin, Z. Wan, S. Xia, S. Jiang, D. Cen, L. Cai, J. Xu, X. Cai, miR-486-3p mediates hepatocellular carcinoma sorafenib resistance by targeting FGFR4 and EGFR, Cell Death Dis. 11 (2020) 250.
[11] J. Yu, A. Li, S.M. Hong, R.H. Hruban, M. Goggins, MicroRNA alterations of pancreatic intraepithelial neoplasias, Clin. Cancer Res. 18 (2012) 981–992.
[12] A.M. ElKhouly, R.A. Youness, M.Z. Gad, MicroRNA-486-5p and microRNA-486-3p: multifaceted pleiotropic mediators in oncological and non-oncological conditions, Noncoding RNA Res 5 (2020) 11–21.
[13] L. Wang, P. Wu, Z. Shen, Q. Yu, Y. Zhang, F. Ye, K. Chen, J. Zhao, An immune checkpoint-based signature predicts prognosis and chemotherapy response for patients with small cell lung cancer, Int. Immunopharm. 117 (2023) 109827.
[14] A. Kula, M. Dawidowicz, S. Mielcarska, P. Kiczmer, H. Skiba, M. Krygier, M. Chrabańska, J. Piecuch, M. Szrot, J. Robotycka, B. Ochman, B. Strzałkowska, Z. Czuba, E. Świętochowska, D. Waniczek, Overexpression and role of HHLA2, a novel immune checkpoint, in colorectal cancer, Int. J. Mol. Sci. 24 (2023).
[15] H. Guo, C. Zhang, X. Tang, T. Zhang, Y. Liu, H. Yu, Y. Li, R. Wang, HHLA2 activates the JAK/STAT signaling pathway by binding to TMIGD2 in hepatocellular carcinoma cells, Inflammation 45 (2022) 1585–1599.
[16] M.D. Robinson, D.J. McCarthy, G.K. Smyth, edgeR: a Bioconductor package for differential expression analysis of digital gene expression data, Bioinformatics 26 (2010) 139–140.
[17] Y. Ru, K.J. Kechris, B. Tabakoff, P. Hoffman, R.A. Radcliffe, R. Bowler, S. Mahaffey, S. Rossi, G.A. Calin, L. Bemis, D. Theodorescu, The multiMiR R package and database: integration of microRNA-target interactions along with their disease and drug associations, Nucleic Acids Res. 42 (2014) e133.
[18] P. Langfelder, S. Horvath, WGCNA: an R package for weighted correlation network analysis, BMC Bioinf. 9 (2008) 559.
[19] Y. An, K.L. Furber, S. Ji, Pseudogenes regulate parental gene expression via ceRNA network, J. Cell Mol. Med. 21 (2017) 185–192.
[20] S. Wang, Y. Xiong, L. Zhao, K. Gu, Y. Li, F. Zhao, J. Li, M. Wang, H. Wang, Z. Tao, T. Wu, Y. Zheng, X. Li, X.S. Liu, UCSCXenaShiny: an R/CRAN package for interactive analysis of UCSC Xena data, Bioinformatics 38 (2022) 527–529.
[21] E.J. Nam, H. Yoon, S.W. Kim, H. Kim, Y.T. Kim, J.H. Kim, J.W. Kim, S. Kim, MicroRNA expression profiles in serous ovarian carcinoma, Clin. Cancer Res. 14 (2008) 2690–2695.
[22] X. Qi, C. Yu, Y. Wang, Y. Lin, B. Shen, Network vulnerability-based and knowledge-guided identification of microRNA biomarkers indicating platinum resistance in high-grade serous ovarian cancer, Clin. Transl. Med. 8 (2019) 28.
[23] Y.Q. Wang, R.D. Guo, R.M. Guo, W. Sheng, L.R. Yin, MicroRNA-182 promotes cell growth, invasion, and chemoresistance by targeting programmed cell death 4 (PDCD4) in human ovarian carcinomas, J. Cell. Biochem. 114 (2013) 1464–1473.
[24] S.K. Dwivedi, S.B. Mustafi, L.S. Mangala, D. Jiang, S. Pradeep, C. Rodriguez-Aguayo, H. Ling, C. Ivan, P. Mukherjee, G.A. Calin, G. Lopez-Berestein, A.K. Sood, R. Bhattacharya, Therapeutic evaluation of microRNA-15a and microRNA-16 in ovarian cancer, Oncotarget 7 (2016) 15093–15104.
[25] C.C. Huang, P.K. Yang, Y.S. Huang, S.U. Chen, Y.S. Yang, M.J. Chen, The role of circulating miRNAs in mechanism of action and prediction of therapeutic responses of metformin in polycystic ovarian syndrome, Fertil. Steril. 119 (2023) 858–868.
[26] P. Sampath, M. Moorthy, A. Menon, L. Madhav, A. Janaki, M. Dhanapal, A.P. Natarajan, S. Hissar, U.D. Ranganathan, G. Ramaswamy, R. Bethunaickan, Downregulation of monocyte miRNAs: implications for immune dysfunction and disease severity in drug-resistant tuberculosis, Front. Immunol. 14 (2023) 1197805.
[27] M.C. Pulanco, A.T. Madsen, A. Tanwar, D.T. Corrigan, X. Zang, Recent advancements in the B7/CD28 immune checkpoint families: new biology and clinical therapeutic strategies, Cell. Mol. Immunol. 20 (2023) 694–713.
[28] L. Wang, X. Wang, X. Zhu, L. Zhong, Q. Jiang, Y. Wang, Q. Tang, Q. Li, C. Zhang, H. Wang, D. Zou, Drug resistance in ovarian cancer: from mechanism to clinical trial, Mol. Cancer 23 (2024) 66.
[29] M. Cui, Y. Liu, L. Cheng, T. Li, Y. Deng, D. Liu, Research progress on anti-ovarian cancer mechanism of miRNA regulating tumor microenvironment, Front. Immunol. 13 (2022) 1050917.
[30] R. Marima, F.Z. Francies, R. Hull, T. Molefi, M. Oyomno, R. Khanyile, S. Mbatha, M. Mabongo, D. Owen Bates, Z. Dlamini, MicroRNA and alternative mRNA splicing events in cancer drug response/resistance: potent therapeutic targets, Biomedicines 9 (2021).
[31] S. Niranjanakumari, E. Lasda, R. Brazas, M.A. Garcia-Blanco, Reversible cross-linking combined with immunoprecipitation to study RNA-protein interactions in vivo, Methods 26 (2002) 182–190.
[32] S.T. Chou, H.Y. Peng, K.C. Mo, Y.M. Hsu, G.H. Wu, J.R. Hsiao, S.F. Lin, H.D. Wang, S.G. Shiah, MicroRNA-486-3p functions as a tumor suppressor in oral cancer by targeting DDR1, J. Exp. Clin. Cancer Res. 38 (2019) 281.
[33] H. Ye, X. Yu, J. Xia, X. Tang, L. Tang, F. Chen, MiR-486-3p targeting ECM1 represses cell proliferation and metastasis in cervical cancer, Biomed. Pharmacother. 80 (2016) 109–114.

[34] M. Wang, C.C. Chao, P.C. Chen, P.I. Liu, Y.C. Yang, C.M. Su, W.C. Huang, C.H. Tang, Thrombospondin enhances RANKL-dependent osteoclastogenesis and facilitates lung cancer bone metastasis, Biochem. Pharmacol. 166 (2019) 23–32.
[35] K.K.W. To, Z. Huang, H. Zhang, C.R. Ashby Jr., L. Fu, Utilizing non-coding RNA-mediated regulation of ATP binding cassette (ABC) transporters to overcome multidrug resistance to cancer chemotherapy, Drug Resist. Updates 73 (2024) 101058.
[36] K. Mortezaee, HHLA2 immune-regulatory roles in cancer, Biomed. Pharmacother. 162 (2023) 114639.
[37] C. Boulhen, S. Ait Ssi, H. Benthami, I. Razzouki, A. Lakhdar, M. Karkouri, A. Badou, TMIGD2 as a potential therapeutic target in glioma patients, Front. Immunol. 14 (2023) 1173518.
[38] N. Woolf, B.E. Pearson, P.A. Bondzie, R.D. Meyer, M. Lavaei, A.C. Belkina, V. Chitalia, N. Rahimi, Targeting tumor multicellular aggregation through IGPR-1 inhibits colon cancer growth and improves chemotherapy, Oncogenesis 6 (2017) e378.
[39] M. Janakiram, J.M. Chinai, S. Fineberg, A. Fiser, C. Montagna, R. Medavarapu, E. Castano, H. Jeon, K.C. Ohaegbulam, R. Zhao, A. Zhao, S.C. Almo, J.A. Sparano, X. Zang, Expression, clinical significance, and receptor identification of the newest B7 family member HHLA2 protein, Clin. Cancer Res. 21 (2015) 2359–2366.